

Peripapillary retinal nerve fiber layer following vessel density correction at different IOP values

Jan Lestak, Martin Fus, Sarka Pitrova

Purpose. The aim of this study was to define the thickness of the retinal nerve fiber layer (RNFL) in the peripapillary region of the retina after adjusting for the effect of vessel density (VD) in patients with pathological intraocular pressure (IOP).

Patients and Methods. 69 patients (122 eyes) with IOP >21 mmHg (range 21–36 mmHg, mean 23.65 ± 2.70 mmHg). 32 were men (average age 55 ± 13 years) and 37 were women (average age 52 ± 14 years). IOP was measured using the Ocular Response Analyser (ORA). VD and RNFL were measured peripapillary by OCT (Avanti RTVue XR) in eight segments: Inferior Temporal – IT (1); Temporal Inferior – TI (2); Temporal Superior – TS (3); Superior Temporal – ST (4); Superior Nasal – SN (5); Nasal Superior – NS (6); Nasal Inferior – NI (7) and Inferior Nasal – IN (8). The VD value was subtracted from the total RNFL value.

Results. A corrected value for the RNFLc nerve fiber layer thickness (RNFLc) was introduced to account for VD across the RNFL volume in each segment. Person's correlation coefficient (r) was used to assess the correlation between IOP and RNFLc. The strongest correlations in RNFLc were in segments 5 ($r = -0.32$, $P = 0.002$) and 8 ($r = -0.21$, $P = 0.037$).

Conclusion: The greatest changes in RNFLc (RNFL minus VD) were in eyes with pathological IOP in segments 5 and 8, the location of the retinal ganglion cell magnocellular fibers. That is, when the thickness of the nerve fiber layer was reduced by correcting for vessel density, there was a significant correlation in segments 5 ($r = -0.32$, $P < 0.05$) and 8 ($r = -0.21$, $P < 0.05$) with intraocular pressure. The results suggest use of a corrected RNFL from VD value as more appropriate for detecting early changes in glaucoma.

Key words: glaucoma, intraocular pressure, optical coherence tomography with angiography, vessel density, ocular hypertension, retinal nerve fiber layer, retinal ganglion magnocellular layer

Received: October 5, 2023; Revised: January 12, 2024; Accepted: January 12, 2024; Available online: January 17, 2024

<https://doi.org/10.5507/bp.2024.001>

© 2025 The Authors; <https://creativecommons.org/licenses/by/4.0/>

Department of Natural Sciences, Faculty of Biomedical Engineering, Czech Technical University in Prague, Kladno 2, Czech Republic
Corresponding author: Jan Lestak, e-mail: lestak@seznam.cz

INTRODUCTION

Glaucoma is defined as an optic neuropathy characterized by changes in the optic nerve target and visual fields¹. This conventional definition is insufficient and could be expanded. For example, in hypertensive glaucoma, there is primary damage to the retinal ganglion cells and then to the entire visual pathway, including the visual cortex². A decisive role is played by high IOP which damages all ganglion cells, but predominantly their magnocellular series^{3–6}.

That the first changes after IOP increase occur in ganglion cells themselves (shrinkage of the dendritic tree and the somata) and that their axons narrow only later was described by Weber et al.⁷. Similarly, Naskar et al. showed experimentally that changes at the level of ganglion cells occur earlier than changes in the axons⁴. This was demonstrated by Soto et al, who found in mouse models that retinal ganglion cell degeneration in glaucoma occurs in two stages. The first involves ganglion cell atrophy and the second, damage to the ganglion cell axons. The retrolaminar degeneration of the axons themselves occurs before that of the intraretinal parts⁸. That these are predominantly magnocellular fibres was confirmed by Quigley et

al – larger diameter fibres died faster than smaller fibres but there was damage in all fibre types⁹.

This implies that the first changes in peripapillary RNFL will occur in segments where magnocellular fibers are located. In a previous publication, the most significant correlation between IOP and RNFL changes was demonstrated in segments 1, 4, 5 and 8 (ref.¹⁰).

The VD rate itself was most significantly correlated with IOP in segments 1, 4, 5, 6, 7 and 8.

After statistical correction of VD from RNFL using the partial correlation coefficient, the most significant correlation was found in segments 5 and 8 (ref.¹¹).

On the basis of a calculation using the partial correlation coefficient, we were interested in whether this result would be consistent with the mathematical subtraction of the VD from the total RNFL value. This was the aim of this study.

MATERIAL AND METHODS

The cohort consisted of 69 subjects (122 eyes), who had IOP >21 (21–36 mmHg), mean value = 23.65 ± 2.7 mmHg measured at the Ophthalmology Clinic JL in

Prague from January to May 2022 in a routine outpatient setting. There were 32 men (6 with one eye examined and 26 with both eyes examined; age range 21–76 years; mean age 55 ± 13 years) and 37 women (4 with one eye examined and 30 with both eyes examined; age range 22–75 years; mean age 52 ± 14 years). Selected criteria included: decimal visual acuity 1.0 with possible correction up to ± 3 diopters, no pathological changes in visual fields and no other ocular or neurological diseases. IOP was measured using a non-contact Ocular Response Analyser II device (Reichert, Inc.) accounting for corneal hysteresis, and the value was determined as the average of three relevant measurements. The visual field was examined by static perimetry with a rapid threshold strategy for glaucoma testing (M 700 automated perimeter; Medmont International Pty Ltd). Original VD and RNFL was measured using the in-built software of the Avanti RTVue XR instrument (version 2018.0.018; Optovue, Inc.) in eight peripapillary segments. The resulting scan images were automatically divided into the following segments: inferior-temporal (IT, segment 1), followed by temporal-inferior (TI, segment 2), temporal-superior (TS, segment 3), superior-temporal (ST, segment 4), superior-nasal (SN, segment 5), nasal-superior (NS, segment 6), nasal-inferior (NI, segment 7) and inferior-nasal (IN, segment 8). The statistical parameters were calculated using the software STATISTICA 12.

The effect of VD on total RNFL thickness was cor-

rected for the percentage distribution of vessels within the entire volume of a given segment as a volume difference, yielding the parameter RNFLc. The resulting value was evaluated in relation to IOP using the Pearson correlation coefficient r divided by segment. The value of r was used to distinguish between: weak ($|r| < 0.3$), moderate ($0.3 < |r| < 0.8$) and strong ($|r| > 0.8$) linear relationships. The study was performed according to the latest Declaration of Helsinki and approved by the internal ethics committee of the Ophthalmology Clinic JL (approval no. OKJL/220806/02; Prague, Czech Republic).

RESULTS

The mean age of the patients was 45 ± 6 years, mean IOP 23.65 ± 2.70 mmHg (21–36 mmHg), overall defect (OD) of visual field was equal to 1.93 ± 1.19 . The mean VD and RNFL and the standard deviation of the whole group in each segment are shown in Table 1. The highest mean VD was identified in segment 1, the same segment as the highest mean RNFL thickness. But for the corrected RNFLc parameter, segments 5 and 8 predominated. The change in RNFL thickness value to RNFLc is demonstrated in Fig. 1.

The correlation between the IOP parameters RNFL, VD and RNFLc of all 122 eyes are shown in Table 2.

Table 1. Mean values and their standard deviations.

	Vessel Density [%]	RNFL thickness [μ m]	RNFLc [μ m]
1-IT	56.44 ± 6.33	139.64 ± 24.85	59.23 ± 10.97
2-TI	52.85 ± 4.02	69.49 ± 12.02	32.25 ± 5
3-TS	55.80 ± 3.58	72.93 ± 12.15	32.24 ± 5.13
4-ST	54.44 ± 6.00	123.07 ± 22.02	55.39 ± 10.42
5-SN	49.36 ± 8.38	127.33 ± 23.33	64.27 ± 10.49
6-NS	48.30 ± 5.13	103.07 ± 16.72	52.88 ± 8.14
7-NI	46.81 ± 5.34	85.69 ± 15.74	45.33 ± 7.13
8-IN	50.66 ± 13.43	129.94 ± 21.99	65.9 ± 11.2

VD (first column), RNFL (second column) and RNFL-VD (third column). IT-inferior temporal segment (1), TI - temporal-inferior (2), TS - temporal-superior (3), ST - superior temporal (4), SN - superior nasal (5), NS - nasal-superior (6), NI - nasal-inferior (7) a IN - inferior-nasal segment (8).

Table 2. Pearson correlation coefficients between IOP and RNFL in each segment (1st column), between IOP and VD (2nd column, results from reference 11) and correlation coefficient between IOP and RNFL after subtraction of VD (3rd column).

segments	Pearson correlation coefficient (n=122)		
	IOP vs. RNFL	IOP vs. VD	IOP vs. RNFLc
1-IT	$-0.23^* (P=0.010)$	$-0.29^* (P=0.001)$	$-0.17 (P=0.090)$
2-TI	$-0.02 (P=0.790)$	$-0.17 (P=0.060)$	$-0.06 (P=0.596)$
3-TS	$-0.04 (P=0.670)$	$-0.10 (P=0.259)$	$-0.05 (P=0.611)$
4-ST	$-0.24^* (P=0.007)$	$-0.33^* (P=0.000)$	$-0.19 (P=0.059)$
5-SN	$-0.31^* (P=0.001)$	$-0.29^* (P=0.060)$	$-0.32^* (P=0.002)$
6-NS	$-0.14 (P=0.117)$	$-0.37^* (P=0.000)$	$-0.08 (P=0.450)$
7-NI	$-0.06 (P=0.532)$	$-0.32^* (P=0.000)$	$-0.03 (P=0.799)$
8-IN	$-0.28^* (P=0.002)$	$-0.23^* (P=0.010)$	$-0.21^* (P=0.037)$

*marked correlations are significant at $P < 0.05$.

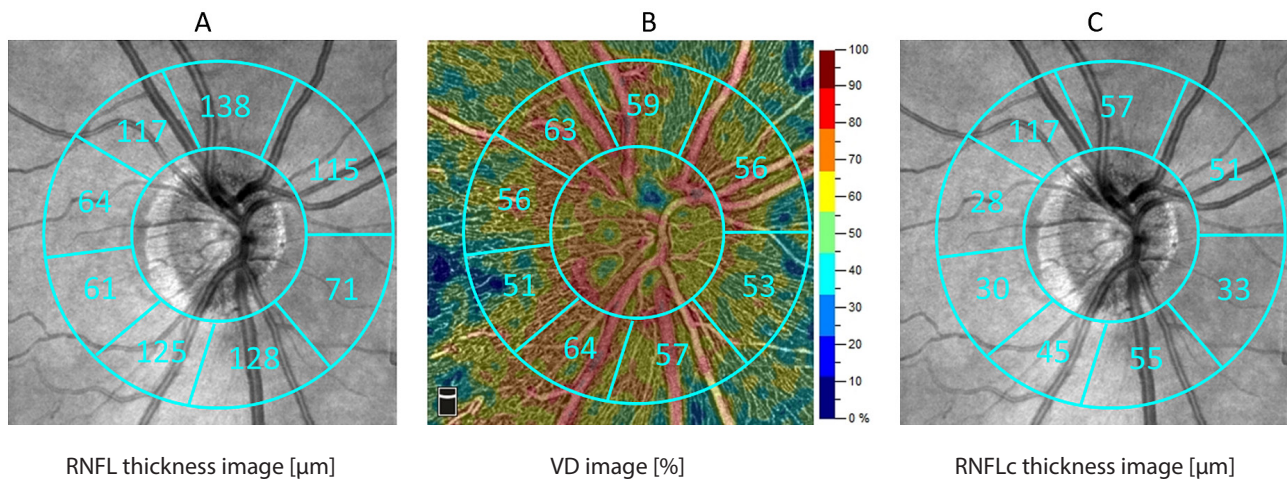


Fig. 1. Demonstration of the resulting RNFLc values after VD correction in individual segments of the right eye. A. original result of RNFL thickness. B. result of VD analyses. C. resulted values after correction – RNFLc.

For all segments, the correlation with IOP was negative. Therefore, it appeared that the higher the IOP value, the lower the RNFL and VD value in each segment. The correlation coefficient table shows that IOP correlates most highly with RNFL in segments 1, 4, 5 and 8. IOP correlates most highly with VD in segments 1, 4, 5, 6, 7 and 8. After subtracting the VD (%) from the RNFL value in each segment, we obtained the “net” RNFLc value, which was compared to the IOP using Pearson’s correlation coefficient by segment. We found the highest correlation in segments 5 ($r=0.32$) and 8 ($r=0.21$), the dominant segments with the highest average corrected RNFLc thickness. According to the correlation coefficient we can distinguish weak ($|r| < 0.3$), moderate ($0.3 < |r| < 0.8$) and strong ($|r| > 0.8$) linear correlations.

DISCUSSION

Ophthalmologists conventionally use average RNFL to make an early diagnosis in cases of hypertensive glaucoma. Due to wide variation however, it is preferable in this instance to focus on selective damage to individual retinal ganglion cells (RGC) fibers which translates to which segment of the retinal peripapillary region is most damaged in the early stages of the disease.

In a previous study, we showed that as IOP increases, VD decreases and the relationship between VD and RNFL increases¹². In patients with IOP below 20 mmHg, we found no relationship between IOP, RNFL and VD (ref.¹²).

That VD play a significant role in RNFL thickness was demonstrated by Hood et al. who found that approximately 13% of total peripapillary RNFL thickness in healthy subjects was attributable to blood vessels¹³.

Similar conclusions were reached by Patel et al. Blood vessels accounted for 9.3% of the total RNFL thickness or area but varied according to their location on the retina. On average, blood vessels comprised 17.6% of the superior and 14.2% of the inferior RNFL, whereas they

accounted for only 2.3% of the areas of the temporal and nasal RNFL (ref.¹⁴).

Allegrini et al. found that the contribution of blood vessels to RNFL thickness was $29.07 \pm 3.945\%$ (ref.¹⁵).

Pereira et al. reported that the circumpapillary distribution of retinal vessels influences RNFL thickness up to 70% (ref.¹⁶). In a previous study, we found a statistically significant correlation between IOP and VD in segments 1, 4, 5, 6, 7 and 8, with the highest correlation found in segment 6 ($r=-0.37$) (ref.¹¹). This is probably due to the larger number of retinal vessels that nourish the inner retinal layers, as the upper nasal quadrant of the retina contains the largest number of ganglion cells¹⁷. Since the vascular component contributes to the total RNFL thickness, we determined the value after subtraction of VD. To eliminate the influence of VD on the total RNFL thickness, we used the relative correlation coefficient in an earlier study. We found statistically significant changes in segments 5 and 8 as in this study but with a difference of significance not in segment 8 ($r=0.39$, $P=0.001$) but in segment 5 ($r=0.32$, $P=0.002$) (ref.¹¹).

In the present study, too we found a statistically significant correlation in segments 5 and 8, except that the higher correlation was not in segment 5 ($P=0.21$) but in segment 8 ($P=0.32$). We think that mathematical subtraction of VD values from total RNFL thickness is more appropriate than using the partial correlation coefficient.

An explanation may be that in this segment is the localization of the fibers of the magnocellular cells, which are three times less in the temporal half of the retina than in the nasal half¹⁷.

Magnocellular retinal cells are morphologically characterized not only by large somata and dendritic tree but also by thicker axons¹⁸. Drenhaus et al. revealed distinct groups of axon diameters with the following mean diameters and proportions. The group of small axons with a diameter of 0.55 micrometer represented 70%. The group of medium-sized axons with a diameter of 1.39 micrometer represented 10% (ref.¹⁹).

The 10% thick axons also correspond to approximately

100 000 retinal magnocellular ganglion cells²⁰. If these are damaged, this is most noticeable in segments 5 or 8, depending on their thickness.

CONCLUSION

When the thickness of the nerve fiber layer was reduced by correcting for vessel density, a significant dependence in the form of a correlation coefficient in segments 5 ($r = -0.32$, $P < 0.05$) and 8 ($r = -0.21$, $P < 0.05$) on the amount of intraocular pressure was demonstrated. Our results suggest the use of corrected RNFL from VD as a more appropriate method for detecting early changes in glaucoma. The above has been filed with the Patent and Invention Office under application number: PV 2023–234.

Author contributions: JL: conceptualization, manuscript writing, patient examination; MF: data evaluation, manuscript writing; SP: manuscript revision, patient examination.

Conflict of interest statement: The authors declare that they have no conflict of interest regarding the publication of this article.

Ethics approval: All details, medical records, figures, medical history or test results were used with the written consent for publication from the patient, which is available from the corresponding author on reasonable request. All data used were anonymized. The present study was performed according to the Declaration of Helsinki and was approved by the internal ethics committee of the Ophthalmology Clinic JL (approval no. OKJL/220806/02; Prague, Czech Republic).

REFERENCES

1. Quigley HA. 21st century glaucoma care. *Eye (Lond)* 2019;33:254–60. doi: 10.1038/s41433-018-0227-8.
2. Lestak J, Fus M. Neuroprotection in glaucoma – a review of electrophysiologist. *Exp Ther Med* 2020;19:2401–05.
3. Morgan JE, Uchida H, Caprioli J. Retinal ganglion cell death in experimental glaucoma. *Br J Ophthalmol* 2000;84:303–10.
4. Naskar R, Wissing M, Thanos S. Detection of Early Neuron Degeneration and Accompanying Microglial Responses in the Retina of a Rat Model of Glaucoma. *Invest Ophthalmol Vis Sci* 2002;43:2962–8.
5. Shou T, Liu J, Wang W, Zhou Y, Zhao K. Differential dendritic shrinkage of alpha and beta retinal ganglion cells in cats with chronic glaucoma. *Invest Ophthalmol Vis Sci* 2003;44:3005–10.
6. Mukai R, Park DH, Okunuki Y, Hasegawa E, Klokman G, Kim CB, Krishnan A, Gregory-Ksander M, Husain D, Miller JW, Connor KM. Mouse model of ocular hypertension with retinal ganglion cell degeneration. *PLoS One* 2019;14(1):e0208713. doi: 10.1371/journal.pone.0208713
7. Weber AJ, Kaufman PL, Hubbard WC. Morphology of single ganglion cells in the glaucomatous primate retina. *Invest Ophthalmol Vis Sci* 1998;39:2304–20.
8. Soto I, Oglesby E, Buckingham BP, et al. Retinal Ganglion Cells Downregulate Gene Expression and Lose Their Axons within the Optic Nerve Head in a Mouse Glaucoma Model *J Neurosci* 2008;28:548–61.
9. Quigley HA, Dunkelberger GR, Green WR. Chronic human glaucoma causing selectively greater loss of large optic nerve fibers. *Ophthalmology* 1988;95:357–63.
10. Lestak J, Fus M, Kral J. Axons of retinal ganglion cells on the optic nerve target at different values of intraocular pressure. *Clin Ophthalmol* 2022;16:3673–9.
11. Lestak J, Fus M, Kral J. Axons of retinal ganglion cells on the optic nerve disc following vessel density correction at different IOP values. *Exp Ther Med* 2023;25(6):261. doi: 10.3892/etm.2023.11960
12. Kral J, Lestak J, Nutterova E. OCT angiography, RNFL and visual field at different values of intraocular pressure. *Biomed Rep* 2022;16:36. doi: 10.3892/br.2022.1519
13. Hood DC, Fortune B, Arthur SN, Xing D, Salant JA, Ritch R, Liebmann JM. Blood vessel contributions to retinal nerve fiber layer thickness profiles measured with optical coherence tomography. *J Glaucoma* 2008;17:519–28.
14. Patel N, Luo X, Wheat JL, Harwerth RS. Retinal Nerve Fiber Layer Assessment: Area versus Thickness Measurements from Elliptical Scans Centered on the Optic Nerve. *Invest Ophthalmol Vis Sci* 2011;52:2477–89.
15. Allegrini D, Montesano G, Fogagnolo P, Pece A, Riva R, Romano MR, Rossetti L. The volume of peripapillary vessels within the retinal nerve fibre layer: an optical coherence tomography angiography study of normal subjects. *Br J Ophthalmol* 2018;102(5):611–21. doi: 10.1136/bjophthalmol-2017-310214
16. Pereira I, Weber S, Holzer S, Resch H, Kiss B, Fischer G, Vass C. Correlation between retinal vessel density profile and circumpapillary RNFL thickness measured with Fourier-domain optical coherence tomography. *Br J Ophthalmol* 2014;98(4):538–43. doi: 10.1136/bjophthalmol-2013-303910
17. Curcio CA, Allen KA. Topography of ganglion cells in human retina. *J Comp Neurol* 1993;300:5–25.
18. Rodieck RW, Binmoeller KF, Dineen J. Parasol and midget ganglion cells of the human retina. *J Comp Neurol* 1985;233:115–32.
19. Drenhaus U, Gunten A, Rager G. Classes of axons and their distribution in the optic nerve of the tree shrew (*Tupaia belangeri*). *Anat Rec* 1997;249:103–16.
20. Skalicky SE. Ocular and Visual Physiology Clinical application. Springer Singapore; 2015.